Nanowires

DOI: 10.1002/ange.201105614

# Solution-Phase Synthesis and Characterization of Single-Crystalline SnSe Nanowires**

*Sheng Liu, Xiaoyang Guo, Mingrun Li, Wen-Hua Zhang,* Xingyuan Liu,* and Can Li**

Tin(II) selenide is an important binary IV–VI semiconductor compound with a wide range of potential applications (e.g. memory switching devices, infrared optoelectronic devices, and anode materials for rechargeable lithium batteries).[1] Bulk SnSe has both an indirect band gap at 0.90 eV and a direct band gap at 1.30 eV.[2] Owing to the quantum confinement effect, tunable band gaps of SnSe nanostructured materials (e.g. thin films and nanocrystals)[1e,3] have been demonstrated, which makes them capable of absorbing a major portion of solar energy. As an earth-abundant, environmentally benign, and chemically stable material, SnSe is placed among the most promising candidates for solar cells.[1e,3c]

Most recently, the interest in the controllable synthesis of colloidal tin chalcogenide (SnX; X = S, Se, Te) nanoparticles (NPs) has grown.[3b,c,4] However, nanowires (NWs) are expected to have properties superior to those of nanoparticles owing to their anisotropic geometry and the exciton confinement in two dimensions.[5] It has been demonstrated that, for photovoltaic applications, high-aspect-ratio nanowires have the potential for enhancement of electron transport owing to their direct electron pathway that does not rely on electron hopping, in contrast to nanoparticles.[6] Furthermore, as remarkably powerful building blocks in nanoscale electronic and optoelectronic devices, the synthesis of versatile semiconductor nanowires with superior controllability in structure and dimension is pivotal for exploiting their device applications.[7] In 2003, Qian and co-workers reported the tentative synthesis of SnSe nanowires with a relatively large mean diameter of 50 nm, but the yield was low and the morphology (including irregular crystals) and purity (including tin oxides) were hard to control.[8] In 2006, Zhao et al. developed a template route to synthesize SnSe nanowires, but only polycrystalline products were obtained after a long reaction time (e.g. 36 h), and a tedious process was required to remove the hard template.[9] To date, high-yield synthesis of monocrystalline SnSe nanowires with relatively small diameters, decent aspect ratios, and good quality has remained a challenge; optical and electrical properties and optoelectronic applications of monocrystalline SnSe nanowires have not been described. We present herein a facile, solution-phase synthetic approach to colloidal SnSe nanowires, which have a mean diameter of approximately 20.8 nm, lengths tunable from hundreds of nanometers to tens of micrometers, and more importantly, a monocrystalline structure. Their optical and electric properties are examined by UV/Vis/NIR spectroscopy, cyclic voltammetry (CV), and transient photocurrent measurements, and a quantum confinement effect is clearly revealed. Furthermore, the fabrication of hybrid solar cells based on a blend of SnSe nanowires and poly(3-hexylthiophene) (P3HT) is demonstrated.

Colloidal SnSe nanowires were prepared from commercially available $Sn[N(SiMe_3)_2]_2$, and trioctylphosphine selenide (TOP-Se) in oleylamine (OLA) or OLA/TOPO (trioctylphosphine oxide) solvent mixture by using monodisperse bismuth nanoparticles[10] to catalyze the nanowire growth through the solution-liquid-solid (SLS) mechanism.[11] In a typical synthesis, an injection solution consisting of $Sn[N(SiMe_3)_2]_2$ (0.2 mmol) and Bi-nanoparticle catalysts (2.4 μmol) in octadecene (ODE, 600 μL) was introduced into a three-neck flask that contained a solution of TOP-Se (0.2 mmol) in OLA (4 g) or TOPO/OLA mixture (3.5 g/2.5 g) at 290 °C. The resulting reaction solution was kept at this temperature for 1–2 min before being cooled to room temperature. The product was cleaned and precipitated using hexane and isopropyl alcohol as the solvent and antisolvent, respectively. Finally the purified nanowires were dispersed in common organic solvents such as toluene.

The scanning electron microscopy (SEM) image in Figure 1a shows the ensemble of randomly aligned SnSe nanowires with lengths exceeding 10 μm. The TEM image in Figure 1b displays smooth nanowires with mean diameters of (20.8 ± 2.2) nm (± 10.6 %), which correlates to the size of monodisperse Bi-nanoparticle catalysts (Figure S1 in the Supporting Information). The frozen Bi-nanoparticle seeds were usually observed at the nanowire tips (see arrows in the

[*] Dr. S. Liu, Prof. W.-H. Zhang, Prof. C. Li
State Key Laboratory of Catalysis, Dalian Institute of Chemical Physics, Chinese Academy of Sciences
Dalian 116023 (China)
and
Dalian National Laboratory for Clean Energy
Dalian 116023 (China)
E-mail: whzhang@dicp.ac.cn
canli@dicp.ac.cn
Prof. M. R. Li
State Key Laboratory of Catalysis, Dalian Institute of Chemical Physics, Chinese Academy of Sciences
Dalian 116023 (China)
Dr. X. Y. Guo, Prof. X. Y. Liu
Key Laboratory of Excited State Processes Changchun Institute of Optics, Fine Mechanics and Physics, Chinese Academy of Sciences
Changchun 130033 (China)
E-mail: liuxy@ciomp.ac.cn

[**] This work was supported by the National Natural Science Foundation of China (NSFC, No. 20873141), "Hundred Talents Program" and the Solar Energy Initiative of the Knowledge Innovation Program of the Chinese Academy of Sciences (Grant. No. KGCX2-YW-395).

Supporting information for this article is available on the WWW under http://dx.doi.org/10.1002/anie.201105614.

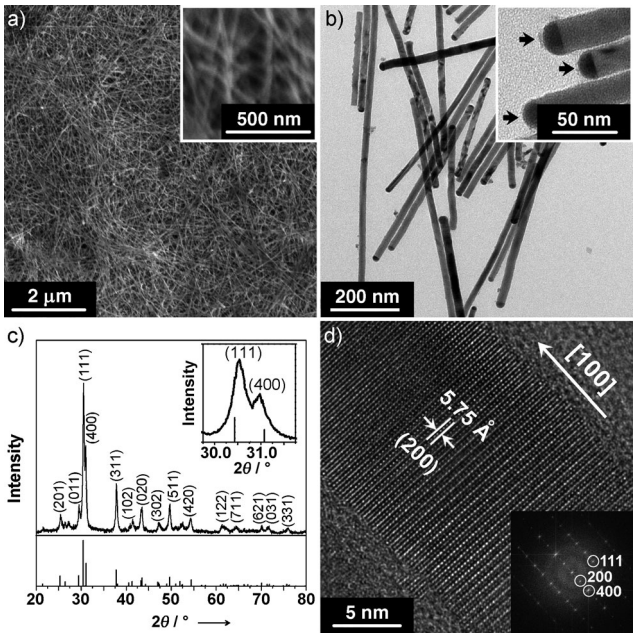


***Figure 1.*** a) SEM image of an ensemble of randomly aligned SnSe nanowires. b) TEM images of the SnSe nanowires. The arrows in the inset point to the frozen droplets of Bi-nanoparticle catalysts at the tips. c) Experimental (top trace) and simulated (lower trace) powder XRD patterns of the SnSe nanowires. The inset XRD pattern is an enlarged view of 30° to 31°. d) HRTEM image of a part of the SnSe nanowire. Inset: FFT of the image, indicating that the nanowire is viewed along the $[0\bar{1}1]$ zone axis of orthorhombic SnSe.

inset of Figure 1b), confirming that the nanowires were formed through the SLS mechanism.[11a] The lengths of SnSe nanowires were easily tuned, ranging from hundreds of nanometers to tens of micrometers, by using different quantities of Bi-nanoparticle catalysts (Figure S2 in the Supporting Information) and different kinds of reaction solvents (Figure S3 in the Supporting Information). As reported for SLS growth of other nanowires,[12] a decrease of the quantity of Bi-nanoparticle catalysts generally led to an increase of nanowire lengths. Meanwhile, the selection of the reaction solvents also influenced the lengths of the nanowires in this study. Acting as both the reaction solvent and the capping ligands, OLA molecules protected the precursors from dissolving into the molten Bi-nanoparticle catalysts because of their well-organized blocking layers on the nanocrystal surfaces.[13] In the neat OLA solvent, the resultant nanowires had smooth surfaces, whereas the maximum lengths were less than several micrometers. Nonetheless, TOPO molecules, as relatively strong and loose capping ligands,[14] could break the dense blocking layers from OLA molecules after partially replacing them, which facilitated the higher supersaturation of the precursors in the vicinity of Bi nanoparticles. Thus, the nanowires synthesized in the TOPO/OLA solvent mixture grew fast and were able to reach lengths of up to tens of micrometers. A detailed discussion on the nanowire synthesis is provided in the Supporting Information.

The powder X-ray diffraction (XRD) pattern of the as-prepared nanowires (Figure 1c) can be indexed to the orthorhombic SnSe structure (JCPDS No. 65-6459, *Pnma*). To understand the growth direction, the microstructures of the SnSe nanowires were further analyzed by high-resolution TEM (HRTEM). Figure 1d reveals the monocrystalline nature of the SnSe nanowires with a lattice distance of 0.575 nm, well-matched to the (200) plane of orthorhombic SnSe. This finding indicates that the growth direction of the SnSe nanowires is oriented along the [100] lattice plane. The fast Fourier transform (FFT) of the image (inset of Figure 1d) further confirms this preferential growth direction of the nanowires. Also, defects such as stacking faults and twins are observed (Figure S2 in the Supporting Information).

The UV/Vis/NIR absorbance spectra of the colloidal SnSe-nanowire suspensions were measured to probe their optical band gaps. The SnSe nanowires absorbed light through the entire visible spectrum to the near IR (Figure 2), thus

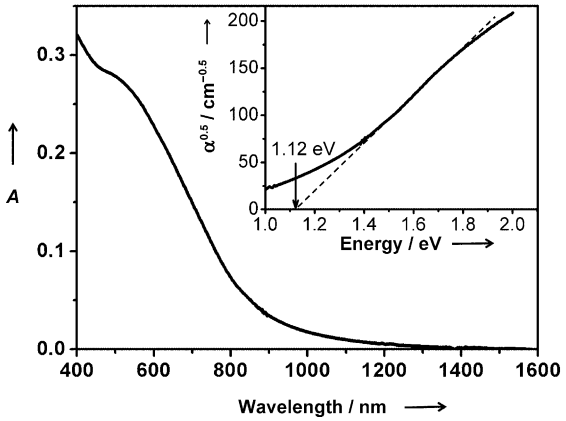


***Figure 2.*** A typical absorption spectrum of the SnSe nanowires (nanowire mean length ca. 1.5 μm, OLA solvent) dispersed in toluene. The square root of the absorption coefficient plotted as a function of energy (inset) displays a linear trend for an indirect transition.

resulting in the black color of this material. The indirect optical bandgap (inset of Figure 2) and direct optical band gap (Figure S6 in the Supporting Information) of typical SnSe nanowires were determined at 1.12 and 1.55 eV, respectively. Both optical band gaps were blue-shifted with respect to those of bulk SnSe.

Thus, the nanowires reported herein are small enough to exhibit apparent quantum confinement effects,[3b,c] and similar results have been found in the nanocrystalline thin films with the average crystal size of 23.3 nm.[1e] Like bulk Si with an indirect band gap of 1.1 eV and CdTe with a direct band gap of 1.5 eV,[11c,15] the band gaps of SnSe nanowires almost perfectly match the distribution of photons in the solar spectrum in terms of optimal conversion to electricity, and thus ideally meet the requirements for solar-cell materials.[16]

To acquire the band structure of SnSe nanowires, CV was employed to investigate the onset reduction potential, which corresponds to the bottom of the conduction band (lowest unoccupied molecular orbital (LUMO)) for semiconductors.[17] To obtain well-defined reduction signals, it was very important to purify the as-prepared nanowires thoroughly. A typical cyclic voltammogram for the nanowire (mean length ca. 1.5 μm) deposited as a thin film on the glassy carbon

  

working electrode is given in Figure 3a. Relative to a $Ag/Ag^+$ reference electrode, the onset reduction potential appears at −1.06 V, which is higher than that of the reported SnSe nanocrystal (−1.4 V).[3b] The bottom of the conduction band

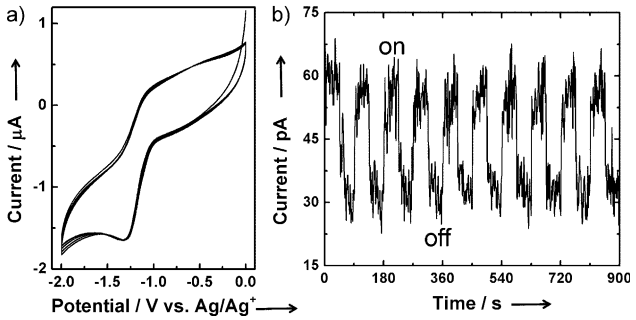


***Figure 3.*** a) Cyclic voltammogram of the SnSe nanowires at a scan rate of 30 $mVs^{-1}$ using a $Ag/Ag^+$ reference electrode. b) Transient photocurrent of the SnSe-nanowire film observed at an applied voltage of 4 V under white-LED illumination (6.42 $mWcm^{-2}$) turned on and off at 45 second intervals.

was determined to be −3.65 eV from vacuum level, as calculated from the onset reduction potential.[18] According to the direct optical band gap of typical SnSe nanowires (1.55 eV), the top of the valence band (highest occupied molecular orbital (HOMO)) was estimated to be at −5.20 eV. Similar results have recently been reported for SnSe nanocrystals.[3b]

To understand the optoelectronic properties of the SnSe nanowires, a nanowire film was prepared by drop-casting a nanowire solution onto two gold electrodes with a separation of approximately 350 μm on a glass substrate.[19] The film was then annealed at 300 °C in vacuum[20] for subsequent photocurrent measurement under illumination with a white-light-emitting diode (LED). The nanowire film was porous, and the nanowires were randomly aligned without noticeable coalescence. The measured dark current at an applied voltage of 4 V was on the order of 30 pA. The relatively weak dark current and the low signal-to-noise ratio were probably due to the unoptimized interconnection in the nanowire network. As shown in Figure 3b, the current quickly increases upon turning on the LED and remains relatively constant during the illumination time (45 s). Upon turning off the LED, the current drops to its pre-illumination value. In contrast to the reported photoelectrical response from oleic acid passivated SnSe nanocrystal films,[3b] the photocurrent-response profile of the SnSe-nanowire films described herein can be reproduced over many cycles (commonly exceeding one hour) without apparent transient photocurrent degradation.

To assess the photovoltaic potentials of the monocrystalline SnSe nanowires used herein, a batch of P3HT/SnSe-nanowires hybrid solar cells with different weight ratios were fabricated in typical sandwich geometry, consisting of ITO/PEDOT:PSS (ca. 30 nm)/P3HT:SnSe nanowires (ca. 80 nm)/LiF (0.5–1 nm)/Al (100 nm; ITO = indium tin oxide, PEDOT = poly(3,4-ethylenedioxythiophene), PSS = poly(styrene-4-sulfonate)). For the best device, the short-circuit current density ($J_{sc}$) of the P3HT/short-SnSe-nanowires hybrid cell (0.046 $mA\,cm^{-2}$) is two times larger than that of the neat P3HT device (0.023 $mA\,cm^{-2}$, Figure 4a), while the open-circuit voltage ($V_{oc}$) increases slightly from 0.50 to 0.54 V and the fill factor (FF) also increases slightly from 0.33

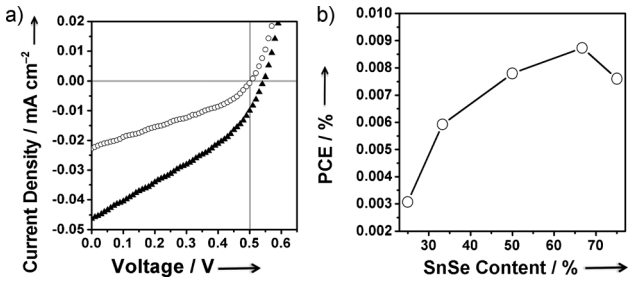


***Figure 4.*** a) Current–voltage (*J*–*V*) characteristics for the P3HT/short-SnSe-NW hybrid cell with P3HT/SnSe weight ratio 1:2 (▲) and the neat P3HT device (○) under 100 $mWcm^{-2}$ of simulated AM 1.5 irradiation. b) Plot of the average PCE as a function of short-SnSe-nanowires content. Note: short nanowires have mean lengths of approximately 1.5 μm.

to 0.35. The obviously enhanced $J_{sc}$ strongly implies that SnSe nanowires have played an important role in the photogeneration of charges and the subsequent transfer of charges from P3HT to SnSe nanowires. Thus, the maximum power conversion efficiency (PCE) is enhanced by 129% (PCE = 0.0087% for 1:2 w/w P3HT/short SnSe nanowires, compared with PCE = 0.0038% for the neat P3HT). The performance of P3HT/short-SnSe-nanowire hybrid cells is dependent on the content of SnSe NWs: the PCE of the hybrid cells increases with the SnSe-nanowire content at the beginning, saturates at a SnSe-nanowire content of approximately 67%, and then decreases upon further increasing the SnSe-nanowire content (Figure 4b). Similarly, the long SnSe nanowires also present a non-monotonic dependence of the average efficiencies on the nanowires/P3HT content ratio (Figure S8 in the Supporting Information). The maximum PCE of the P3HT/long-SnSe-nanowires hybrid cells exhibits an improvement by 174% in comparison with the neat P3HT device, while the open-circuit voltage ($V_{oc}$) and fill factor (FF) remain almost comparable (PCE = 0.0104% for 2:1 w/w P3HT/SnSe nanowires).

In summary, an efficient solution-phase synthetic approach was developed to prepare SnSe nanowires. The nanowires were monocrystalline and exhibited controllable lengths and quantum confinement effects. Furthermore, their optical band gaps, the bottom of the conduction band (LUMO), and the photocurrent properties were studied. These results may improve our understanding of their basic optical and electrical properties and may also aid their utility as building block in various applications, such as photovoltaic devices. The hybrid solar cells based on a blend of the long SnSe nanowires and P3HT exhibited PCEs of 0.01% under AM 1.5 sun. Further studies for enhancing the device performance are under way.

  

## Experimental Section

In a typical synthesis, OLA (4 g) or TOPO/OLA mixture (3.5 g/2.5 g) was placed into a 50 mL three-neck round-bottomed flask, degassed, and dried under vacuum for 30 min at 100 °C. The reaction vessel was then backfilled with $N_2$, and the TOP-Se stock solution (400 μL) was injected into the mixture without exposure to air. The reaction mixture was heated to the desired temperature, typically 290 °C. Separately, $[Sn[N(SiMe_3)_2]_2$ (78 μL, 0.2 mmol) and Bi-nanoparticle stock solution (60 mg, 2.4 μmol) were mixed with ODE (600 μL) inside a glove box to form the tin(II) injection solution. Under vigorous stirring, the tin(II) injection solution was swiftly injected into the reaction mixture to initiate the reaction. After injection the temperature first dropped to 270 °C and a rapid color change occurred. Subsequently, the solution was heated back to 290 °C in about 30–60 s and allowed to react for additional 60 s with constant stirring to produce a black solution. Subsequently, the solution was allowed to cool to room temperature. A hexane/isopropyl alcohol mixture (1:1) was then added to the crude solution, and the nanowires were isolated by centrifugation. The nanowires were additionally purified twice by redispersing them in hexane and precipitating with isopropyl alcohol. Finally, the purified nanowires were dispersed in common organic solvents such as toluene.

Received: August 8, 2011
Published online: October 20, 2011

**Keywords:** nanostructures · photophysics · solar cells · synthetic methods

[1] a) D. Chun, R. M. Walser, R. W. Bene, T. H. Courtney, *Appl. Phys. Lett.* **1974**, *24*, 479 – 481; b) M. Z. Xue, J. Yao, S. C. Cheng, Z. W. Fu, *J. Electrochem. Soc.* **2006**, *153*, A270 – A274; c) A. Agarwal, M. N. Vashi, D. Lakshminarayana, N. M. Batra, *J. Mater. Sci. Mater. Electron.* **2000**, *11*, 67 – 71; d) N. D. Boscher, C. J. Carmalt, R. G. Palgrave, I. P. Parkin, *Thin Solid Films* **2008**, *516*, 4750 – 4757; e) B. Pejova, I. Grozdanov, *Thin Solid Films* **2007**, *515*, 5203 – 5211; f) Z. Zainal, S. Nagalingam, A. Kassim, M. Z. Hussein, W. M. M. Yunus, *Sol. Energy Mater. Sol. Cells* **2004**, *81*, 261 – 268; g) B. Subramanian, C. Sanjeeviraja, M. Jayachandran, *J. Cryst. Growth* **2002**, *234*, 421 – 426; h) B. Subramanian, T. Mahalingam, C. Sanjeeviraja, M. Jayachandran, M. J. Chockalingam, *Thin Solid Films* **1999**, *357*, 119 – 124; i) A. Agarwal, *J. Cryst. Growth* **1998**, *183*, 347 – 351; j) T. S. Rao, A. K. Chaudhuri, *Bull. Mater. Sci.* **1996**, *19*, 449 – 453.

[2] I. Lefebvre, M. A. Szymanski, J. Olivier-Fourcade, J. C. Jumas, *Phys. Rev. B* **1998**, *58*, 1896 – 1906.

[3] a) B. Pejova, A. Tanusevski, *J. Phys. Chem. C* **2008**, *112*, 3525 – 3537; b) W. J. Baumgardner, J. J. Choi, Y. F. Lim, T. Hanrath, *J. Am. Chem. Soc.* **2010**, *132*, 9519 – 9521; c) M. A. Franzman, C. W. Schlenker, M. E. Thompson, R. L. Brutchey, *J. Am. Chem. Soc.* **2010**, *132*, 4060 – 4061.

[4] a) S. Schlecht, M. Budde, L. Kienle, *Inorg. Chem.* **2002**, *41*, 6001 – 6005; b) S. G. Hickey, C. Waurisch, B. Rellinghaus, A. Eychmuller, *J. Am. Chem. Soc.* **2008**, *130*, 14978 – 14980; c) M. V. Kovalenko, W. Heiss, E. V. Shevchenko, J. S. Lee, H. Schwinghammer, A. P. Alivisatos, D. V. Talapin, *J. Am. Chem. Soc.* **2007**, *129*, 11354 – 11355; d) Y. Xu, N. Al-Salim, C. W. Bumby, R. D. Tilley, *J. Am. Chem. Soc.* **2009**, *131*, 15990 – 15991.

[5] a) M. Law, J. Goldberger, P. D. Yang, *Annu. Rev. Mater. Res.* **2004**, *34*, 83 – 122; b) J. Weber, R. Singhal, S. Zekri, A. Kumar, *Int. Mater. Rev.* **2008**, *53*, 235 – 255; c) D. S. Wang, C. H. Hao, W. Zheng, Q. Peng, T. H. Wang, Z. M. Liao, D. P. Yu, Y. D. Li, *Adv. Mater.* **2008**, *20*, 2628 – 2632.

[6] S. Ren, N. Zhao, S. C. Crawford, M. Tambe, V. Bulović, S. Gradečak, *Nano Lett.* **2011**, *11*, 408 – 413.

[7] a) Y. Li, F. Qian, J. Xiang, C. M. Lieber, *Mater. Today* **2006**, *9*, 18 – 27; b) F. Patolsky, B. P. Timko, G. F. Zheng, C. M. Lieber, *MRS Bull.* **2007**, *32*, 142 – 149; c) H. J. Fan, P. Werner, M. Zacharias, *Small* **2006**, *2*, 700 – 717.

[8] G. Shen, D. Chen, X. Jiang, K. Tang, Y. Liu, Y. Qian, *Chem. Lett.* **2003**, *32*, 426 – 427.

[9] L. L. Zhao, M. Yosef, M. Steinhart, P. Goring, H. Hofmeister, U. Gosele, S. Schlecht, *Angew. Chem.* **2006**, *118*, 317 – 321; *Angew. Chem. Int. Ed.* **2006**, *45*, 311 – 315.

[10] F. D. Wang, R. Tang, H. Yu, P. C. Gibbons, W. E. Buhro, *Chem. Mater.* **2008**, *20*, 3656 – 3662.

[11] a) T. J. Trentler, K. M. Hickman, S. C. Goel, A. M. Viano, P. C. Gibbons, W. E. Buhro, *Science* **1995**, *270*, 1791 – 1794; b) F. D. Wang, A. G. Dong, J. W. Sun, R. Tang, H. Yu, W. E. Buhro, *Inorg. Chem.* **2006**, *45*, 7511 – 7521; c) J. D. Holmes, K. P. Johnston, R. C. Doty, B. A. Korgel, *Science* **2000**, *287*, 1471 – 1473.

[12] F. Wang, W. E. Buhro, *Small* **2010**, *6*, 573 – 581.

[13] a) Z. Li, A. Kornowski, A. Myalitsin, A. Mews, *Small* **2008**, *4*, 1698 – 1702; b) C. Wang, Y. Hou, J. Kim, S. Sun, *Angew. Chem.* **2007**, *119*, 6449 – 6451; *Angew. Chem. Int. Ed.* **2007**, *46*, 6333 – 6335.

[14] X. M. Lu, H. Y. Tuan, J. Y. Chen, Z. Y. Li, B. A. Korgel, Y. N. Xia, *J. Am. Chem. Soc.* **2007**, *129*, 1733 – 1742.

[15] J. D. Beach, B. E. McCandless, *MRS Bull.* **2007**, *32*, 225 – 229.

[16] A. Goetzberger, C. Hebling, H. W. Schock, *Mater. Sci. Eng. R* **2003**, *40*, 1 – 46.

[17] a) S. K. Haram, B. M. Quinn, A. J. Bard, *J. Am. Chem. Soc.* **2001**, *123*, 8860 – 8861; b) Y. Bae, N. Myung, A. J. Bard, *Nano Lett.* **2004**, *4*, 1153 – 1161.

[18] Y. He, H. Y. Chen, J. Hou, Y. Li, *J. Am. Chem. Soc.* **2010**, *132*, 1377 – 1382.

[19] T. Gao, Q. H. Li, T. H. Wang, *Chem. Mater.* **2005**, *17*, 887 – 892.

[20] Q. Y. Yan, H. Chen, W. W. Zhou, H. H. Hng, F. Y. C. Boey, J. Ma, *Chem. Mater.* **2008**, *20*, 6298 – 6300.